



**HAL**  
open science

## Sulfur transformations during two-stage anaerobic digestion and intermediate thermal hydrolysis

F. Forouzanmehr, K. Solon, V. Maisonnave, O. Daniel, E.I.P. Volcke, Sylvie Gillot, Pierre Buffière

► **To cite this version:**

F. Forouzanmehr, K. Solon, V. Maisonnave, O. Daniel, E.I.P. Volcke, et al.. Sulfur transformations during two-stage anaerobic digestion and intermediate thermal hydrolysis. *Science of the Total Environment*, 2022, 810, pp.151247. 10.1016/j.scitotenv.2021.151247 . hal-03801046

**HAL Id: hal-03801046**

**<https://hal.inrae.fr/hal-03801046v1>**

Submitted on 22 Jul 2024

**HAL** is a multi-disciplinary open access archive for the deposit and dissemination of scientific research documents, whether they are published or not. The documents may come from teaching and research institutions in France or abroad, or from public or private research centers.

L'archive ouverte pluridisciplinaire **HAL**, est destinée au dépôt et à la diffusion de documents scientifiques de niveau recherche, publiés ou non, émanant des établissements d'enseignement et de recherche français ou étrangers, des laboratoires publics ou privés.



Distributed under a Creative Commons Attribution - NonCommercial 4.0 International License

1 **Title: Sulfur transformations during two-stage anaerobic digestion and intermediate thermal**  
2 **hydrolysis**

3 *F. Forouzanmehr*<sup>a,b,c</sup>, *K. Solon*<sup>b</sup>, *V. Maisonnave*<sup>c</sup>, *O. Daniel*<sup>c</sup>, *E. I. P. Volcke*<sup>b</sup>, *S. Gillot*<sup>d</sup>, *P.*  
4 *Buffiere*<sup>d\*</sup> <sup>a</sup> Univ Lyon, INSA Lyon, DEEP EA7429, 69621 Villeurbanne, France

5 <sup>b</sup> BioCo Research Group, Department of Green Chemistry and Technology, Ghent University,  
6 Belgium

7 <sup>c</sup> Veolia Research & Innovation (VeRI), Maisons-Laffitte, France

8 <sup>d</sup> INRAE, UR REVERSAAL, F-69625, Villeurbanne Cedex, France

9 \* Corresponding author. E-mail address: [Pierre.Buffiere@insa-lyon.fr](mailto:Pierre.Buffiere@insa-lyon.fr) (Pierre Buffiere)

10

11 **Abstract**

12 The formation of hydrogen sulfide (H<sub>2</sub>S) during anaerobic digestion (AD) imposes constraints on the  
13 valorisation of biogas. So far, inorganic sulfur compounds -mainly sulfate - have been considered as  
14 the main contributors to H<sub>2</sub>S formation, while the contribution of organic sulfur compounds is mostly  
15 neglected. This study investigates the fate of organic and inorganic sulfur compounds during two-stage  
16 anaerobic digestion with intermediate thermal hydrolysis for treatment of primary and secondary  
17 sludge in a WWTP treating domestic wastewater. The results of a seven-week monitoring campaign  
18 showed an overall decrease of organic sulfur compounds in both stages of anaerobic digestion. Further  
19 fractionation of organic sulfur revealed a high conversion of the particulate organic fraction during the  
20 first digestion stage and of the soluble organic fraction during the second digestion stage. The decrease  
21 of soluble organic sulfur during the second digestion stage was attributed to the solubilisation and  
22 hydrolysis of sulfur-containing organic compounds during thermal hydrolysis. In both digestion  
23 stages, more organic sulfur was taken up than particulate inorganic sulfur (metal sulfide) was  
24 produced, indicating the formation of other reduced sulfur forms (e.g. H<sub>2</sub>S). Further batch experiments  
25 confirmed the role of organic sulfur uptake in the formation of H<sub>2</sub>S during anaerobic digestion as

26 sulfate reduction only partly explained the total sulfide formed ( $\text{H}_2\text{S}$  in biogas and precipitated  $\text{FeS}$ ).  
27 Overall, the conversion of organic sulfur was demonstrated to play a major role in  $\text{H}_2\text{S}$  formation (and  
28 thus the biogas quality), especially in case of thermal hydrolysis pretreatment.

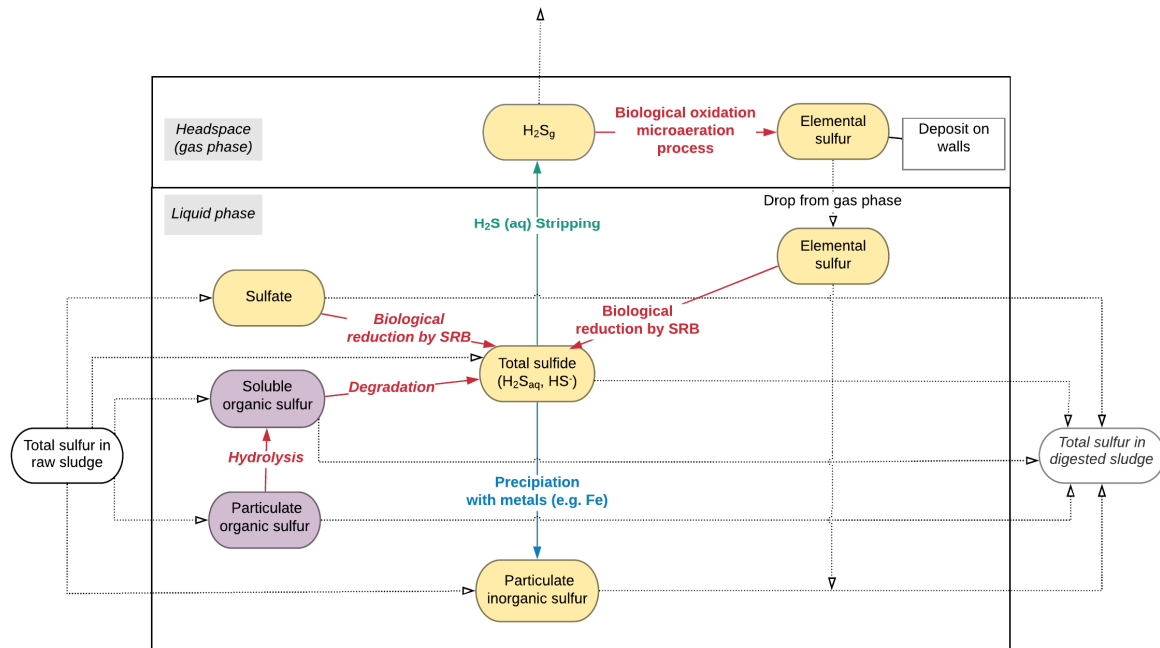
29 Key words: Anaerobic digestion; Intermediate thermal hydrolysis;  $\text{H}_2\text{S}$  formation; organic sulfur;  
30 biological sulfate reduction

## 31 **1 Introduction**

32 Anaerobic digestion has a crucial part in modern wastewater treatment plants (WWTPs). Its primary  
33 role is the stabilisation of waste sludge and the reduction of its volume, by transforming organic matter  
34 in the absence of oxygen. In addition, biogas is produced, which has a high calorific value and is  
35 considered a renewable energy source (Appels et al., 2008). In WWTPs, biogas is used to generate  
36 electricity and heat in combined heat and power (CHP) units, or purified for direct injection into the  
37 natural gas grid. However, the inevitable presence of  $\text{H}_2\text{S}$  in biogas is problematic causing severe  
38 corrosion of electrical equipment, release of sulfur dioxide ( $\text{SO}_2$ ) in cogeneration and boilers, and  
39 entailing other operational, health and safety problems, which necessitates its removal from the biogas.  
40 Therefore, a good process understanding of how sulfur is transformed to  $\text{H}_2\text{S}$  is important to be able to  
41 design appropriate control strategies to decrease  $\text{H}_2\text{S}$  in biogas to low levels.

42 There are three main chemical forms of sulfur existing in sludge: organic sulfur, soluble and insoluble  
43 sulfide and sulfate (Yang et al., 2016). Sulfur is a building block of amino acids and hence presents in  
44 proteins, which are the largest fraction of wastewater organic material (Wilson and Novak, 2009). The  
45 total sulfur composition of sludge in the anaerobic digesters of WWTPs in 10 cities in the United  
46 States of America was composed predominantly of S-containing amino acids (Sommers et al., 1977).  
47 Sulfur species undergo biological, chemical and physical reactions during anaerobic digestion process  
48 (Fig. 1). Degradable particulate organic sulfur would be converted to soluble organic sulfur in form of  
49 soluble protein and amino acids through hydrolysis and further degraded into  $\text{H}_2\text{S}$  and volatile organic  
50 sulfur compounds (Du and Parker, 2013). The reduction of sulfate by sulfate reducing bacteria (SRB)  
51 is another reaction leading to formation of  $\text{H}_2\text{S}$ . SRBs use sulfate as electron donor and VFAs and  $\text{H}_2$

52 as their substrates to produce  $H_2S$ . Dissolved sulfide produced can be transferred to the gas phase as  
 53  $H_2S$ , or remain in the liquid and precipitate as metal sulfide. When microaeration (i.e. dosing small  
 54 amounts of oxygen or air into the anaerobic digester) is applied to the gas phase,  $H_2S$  in the biogas is  
 55 biologically oxidised to elemental sulfur by sulfide oxidising bacteria (Krayzelova et al., 2014).



56  
 57 Fig.1: Sulfur species conversions during anaerobic digestion. Biological, chemical and physical  
 58 reactions are indicated by red, green and blue colours. Organic and inorganic sulfur species are  
 59 specified by yellow and purple colours. The dashed line shows the distribution of total sulfur in the  
 60 raw sludge entering anaerobic digestion, and the composition of total sulfur in the digested sludge.

61 In anaerobic digestion, the formation of  $H_2S$  from biological sulfate reduction has been well  
 62 established. In addition to experimental investigations, the inorganic sulfur reactions have been  
 63 incorporated into mathematical models of anaerobic digestion process (Barrera et al., 2015; D'Acunto  
 64 et al., 2011; Fedorovich et al., 2003; Flores-Alsina et al., 2016; Hauduc et al., 2018; Poinapen and  
 65 Ekama, 2010; Solon et al., 2017). In these studies, the sulfur reactions typically entails microbial  
 66 kinetics for SRB groups, ionic speciation of sulfate and  $H_2S$  and liquid to gas mass transfer of  $H_2S$   
 67 (Ahmed and Rodríguez, 2018). To include the interaction between sulfur, iron and phosphorus, some  
 68 models have considered additional reactions such as precipitation of ferrous iron with sulfide as  $FeS$ ,

69 chemical reduction of ferric iron to ferrous iron using sulfide as electron donor and release of iron  
70 phosphate with sulfide (Flores-Alsina et al., 2016; Hauduc et al., 2018; Solon et al., 2017).

71 On the other hand, the formation of H<sub>2</sub>S originating from degradation of organic sulfur during  
72 anaerobic digestion has been given less attention compared to biological sulfate reduction. This could  
73 be explained by the fact that majority of experimental and modelling studies focused on sulfate-rich  
74 wastewaters (Barrera et al., 2013; Fedorovich et al., 2003; Visser, 1995). On the contrary, sludge  
75 originating from municipal WWTPs is composed predominantly of organic sulfur (Sommers et al.,  
76 1977). In a recent study, Erdirencelebi and Kucukhemek (2018) observed a strong correlation between  
77 the organic solids in primary sludge and H<sub>2</sub>S concentration in biogas of full-scale anaerobic digesters  
78 over a long period. They suggested that hydrolysis of the proteinaceous matters in primary sludge was  
79 the major source of dissolved and gaseous hydrogen sulfide.

80 The application of sludge pretreatment techniques, as a successful method to increase the  
81 biodegradability of sludge, has increased to overcome the main limiting factor of the anaerobic  
82 digestion process, i.e. hydrolysis (Appels et al., 2008; Barber, 2016). Thermal hydrolysis can either be  
83 applied as a pretreatment step (usually for secondary sludge) or intermediate treatment for the digested  
84 sludge (Remy and Diercks, 2016). Recently, the total sulfur mass flow analysis in a municipal WWTP  
85 indicated high H<sub>2</sub>S mass flows in biogas of anaerobic digester located after thermal hydrolysis  
86 (Forouzanmehr et al., 2021) Studying the impact of sludge thermal treatment on the sulfur cycle and  
87 formation of H<sub>2</sub>S in the subsequent anaerobic digestion is still relatively unexplored in the literature.

88 At present, there is a lack of quantitative information on the formation of H<sub>2</sub>S in full-scale municipal  
89 anaerobic digesters. In this study, first the operational performance of a full-scale Digestion – Lysis –  
90 Digestion (DLD) process configuration was evaluated. Next, total sulfur content and fractionation of  
91 sulfur species in feed and digested sludge of both digestion stages were obtained using long-term  
92 collected data. The influence of intermediate thermal hydrolysis on the solubilisation of organic matter  
93 and sulfur was especially examined. Furthermore, the contribution of biological sulfate reduction to  
94 the formation of H<sub>2</sub>S was monitored in lab-scale anaerobic digestion experiments. The latter were also  
95 used to analyse the profile of H<sub>2</sub>S production and methane yield for the two stages of sludge treatment.

## 96 **2 Material and methods**

### 97 **2.1 WWTP under study**

98 The municipal WWTP under study has a capacity of 620,000 P.E. and comprises primary treatment  
99 and secondary treatment. The secondary treatment is based on an integrated fixed-film activated  
100 sludge (IFAS) process for the removal of carbon, nitrogen and phosphorus. During intense rain events,  
101 the potential surplus influent wastewater flow is directed towards the rain treatment line which is  
102 based on chemically enhanced primary treatment. The raw sludge is composed mainly of primary  
103 sludge and secondary sludge and a smaller contribution (~6%) from sludge produced during the rain  
104 treatment line. The latter contains iron due to the usage of iron chloride for chemical phosphorus  
105 removal in the rain treatment line. The sludge treatment is performed in a Digestion – Lysis –  
106 Digestion (DLD) process configuration. The first stage of anaerobic digestion takes place in two  
107 parallel units (D1a and D1b). The first-stage digested sludge is then dewatered in a centrifuge and sent  
108 to a thermal hydrolysis unit (165°C, 8 bars, 30 minutes). The thermally treated sludge is diluted and  
109 cooled by adding some treated WWTP effluent. The subsequent second digestion stage (D2) is  
110 performed in a single unit. All three mesophilic digester tanks have the same volume (6100 m<sup>3</sup>) and  
111 are equipped with air injectors to the headspace for the removal of hydrogen sulfide from the biogas  
112 through microaeration. The process flow diagram of the whole plant under study are presented in  
113 Supplementary Information (section A1).

### 114 **2.2 Measurement campaign**

#### 115 **2.2.1 Sampling strategy**

116 The operational data for the anaerobic digesters including sludge flow rates, sludge dry solids (DS)  
117 and volatile solids (VS) measurements, biogas flow rate and methane concentrations were obtained on  
118 a daily basis from historical data between January 2018 to November 2020. These data were used to  
119 assess long-term overall performance of the anaerobic digesters in terms of hydraulic retention time  
120 (HRT), daily volatile solids load, volatile solids reduction, biogas production and methane yield.

121 In addition to the routine data, dedicated measurement campaigns were performed. The first  
122 measurement campaign (C1) was conducted over seven weeks between May and July 2018 to  
123 determine the various sulfur fractions throughout the sludge treatment line. Grab samples were taken  
124 from first stage and second digestion stage. Approximately 1-3 samples per week were taken. Samples  
125 were analysed for total sulfur, DS and VS. The second measurement campaign (C2) took place over  
126 two weeks in June 2019. Grab samples were taken from the same sampling points as in C1, and were  
127 analysed for total sulfur and dry solids. The third measurement campaign (C3) was done on October  
128 22<sup>nd</sup> 2020. Grab samples were collected from inlet and outlet of first stage digestion, thermal  
129 hydrolysis and second digestion stages. Anaerobic digestion batch experiments were performed on  
130 these samples (except outlet of the first digester) in order to assess and quantify the methane and the  
131 H<sub>2</sub>S production (section 2.3). The collected samples were also analysed for total sulfur, sulfate, soluble  
132 iron, soluble and total COD and VFAs. The overview of these measurement campaigns including  
133 sampling points, type and number of measurements are provided in Supplementary Information  
134 (section A2).

### 135 **2.2.2 Measurement protocols**

136 DS and VS were measured by mass difference after drying (105°C) and calcination (550°C) of the  
137 samples. Total sulfur and iron were measured using ICP method. Sulfate was measured by ion  
138 chromatography. Reactor digestion method (Hach® method) was used to measure soluble COD and  
139 the total COD in C1 and C2, while the analysis of total COD in C3 was done using an internal method  
140 based on standard NF U 44-161 and NF ISO 142352, which is described as acid digestion with H<sub>2</sub>SO<sub>4</sub>  
141 in the presence of K<sub>2</sub>Cr<sub>2</sub>O<sub>7</sub> and the reading by UV at 585nm. VFAs were measured by ion  
142 chromatography.

143 Total sulfur was measured on raw sample, while the soluble and particulate fractions were determined  
144 after centrifugation and filtration. Inorganic sulfur was obtained by performing total sulfur analysis on  
145 the residuals of calcination of the raw and particulate samples at 550°C. From these measurements  
146 other sulfur fractionation was calculated by following equations:

$$147 \text{ Organic sulfur fraction (OSF)} = (S_{\text{Total}} - S_{\text{Inorganic}}) / S_{\text{Total}} \quad \text{Eq. (1)}$$

148 Particulate organic sulfur fraction (POSF) =  $(S_{\text{Particulate}} - S_{\text{Particulate\_Inorganic}})/S_{\text{Particulate}}$  Eq. (2)

149  $S_{\text{Particulate\_Organic}} = \text{POSF} \times S_{\text{Particulate}}$  Eq. (3)

150  $S_{\text{Soluble\_Organic}} = \text{OSF} \times S_{\text{Total}} - S_{\text{Particulate\_Organic}}$  Eq. (4)

151  $S_{\text{Soluble\_Inorganic}} = S_{\text{Soluble}} - S_{\text{Soluble\_Organic}}$  Eq. (5)

152 In this characterisation, total sulfur is divided into soluble ( $S_{\text{Soluble}}$ ) and particulate ( $S_{\text{Particulate}}$ ) fractions.  
153 Further, each fraction is divided into organic ( $S_{\text{Particulate\_Organic}}$  and  $S_{\text{Soluble\_Organic}}$ ) and inorganic  
154 ( $S_{\text{Particulate\_Inorganic}}$  and  $S_{\text{Soluble\_Inorganic}}$ ) fractions. It is assumed that particulate inorganic sulfur consisted  
155 of heavy metal sulfides. Particulate organic sulfur was assumed to be sulfur bound in particulate  
156 organic matter. Soluble sulfur was assumed to consist of dissolved and colloidal sulfur-containing  
157 compounds such as soluble proteins, amino acids, sulfide and sulfate Du and Parker (2013).

### 158 **2.3 Batch tests**

159 Anaerobic digestion batch tests were performed on samples taken from inlet and outlet of the  
160 anaerobic digesters and thermal hydrolysis process. These tests were carried out in 1-L glass bottles at  
161 35 °C to measure the methane yield and evaluate the contribution of biological sulfate reduction to  
162 sulfide production.

163 The tests were performed according to the biochemical methane potential (BMP) guidelines provided  
164 by a dedicated international working group (Holliger et al., 2016). Substrate to Inoculum ratio (S/I)  
165 was 0.5 on a VS basis. The substrates were collected from the inlet of the first stage digester, inlet and  
166 outlet of thermal hydrolysis unit, and outlet of second stage digester. Each reactor was flushed with  
167 nitrogen for at least 3 minutes to ensure anaerobic conditions. For all samples, the test was performed  
168 in triplicates. Three blank tests containing only inoculum were incubated simultaneously to correct for  
169 the methane and H<sub>2</sub>S produced by the inoculum. The digestion experiments were run for  
170 approximately 30 days. The biogas production was determined with the manometric method (Amodeo  
171 et al., 2020). The biogas composition was measured by gas chromatography using an Agilent 3000  
172 micro gas chromatograph, equipped with a thermal conductivity detector (GC-TCD). Molsieve 5A (14  
173 m length; pore size: 5 Å) and PoraPlotA (10 m length; 0.320mm ID) columns were used as stationary

174 phases for GC-TCD, with Argon and Helium as carrier gases, respectively. The micro-GC was  
 175 calibrated for H<sub>2</sub>, H<sub>2</sub>S, CO<sub>2</sub>, CH<sub>4</sub>, O<sub>2</sub> and N<sub>2</sub>. Methane and hydrogen sulfide production were  
 176 calculated in STP conditions (0°C, 101325 Pa) after correction for moisture. At the end of each batch  
 177 test, the digested sludge was analysed for total sulfur, soluble sulfur, and sulfate.

178 The contribution of biological sulfate reduction to formation of H<sub>2</sub>S was calculated by the difference  
 179 between initial and final sulfate concentrations. Produced sulfide in these experiments was the sum of  
 180 H<sub>2</sub>S in biogas and precipitated sulfide as FeS. Precipitated sulfide as FeS was estimated based on the  
 181 difference between initial and final soluble iron concentrations. It is important to bear in mind that  
 182 other forms of sulfide (e.g. soluble sulfide remained in effluent and precipitated sulfide with other  
 183 metals) were not included; therefore, produced sulfide value could be lower than the total sulfide.

### 184 **3 Results**

#### 185 **3.1 Long-term operation of anaerobic digesters**

186 The two parallel first-stage digesters (D1a and D1b) were operated under similar conditions (Table 1):  
 187 an HRT of 21 days and a VS load of 11011 and 11278 kg VS/day for D1a and D1b, respectively.  
 188 Their operational performance was also very comparable: a VS reduction of 39% and 41% and a mean  
 189 methane yield of  $279 \pm 54$  and  $316 \pm 65$  mL CH<sub>4</sub>/g VS<sub>in</sub>, for D1a and D1b, respectively. These  
 190 methane yield values were in agreement with the value obtained from batch experiments, which was  
 191 performed on a grab sample of D1<sub>feed</sub> taken in 2020. As the main operational variables of D1a and D1b  
 192 indicate similar operating conditions and performance, only one of them – in this case D1a - was  
 193 considered for the study of sulfur transformations.

194 **Table 1:** Summary of overall mean values and standard deviations of operational parameters of the  
 195 first stage digesters (D1a and D1b) and the second stage digester (D2), obtained from daily  
 196 measurements between January 2018 to November 2020.

Parameter		First stage		Second stage
		D1a	D1b	D2
HRT	day	21 ± 2	21 ± 3	31 ± 6
Daily VS load	kg VS/day	11011 ± 1708	11278 ± 1774	9610 ± 1798
VS reduction (VSR) <sup>1</sup>	%	39 ± 5	41 ± 5	32 ± 5

Daily biogas production	Nm <sup>3</sup> /d	5163 ± 1185	6012 ± 1302	6162 ± 1585
Methane yield	mL CH <sub>4</sub> /g VS <sub>in</sub>	279 ± 54	316 ± 65	379 ± 66
Methane yield of BMP test <sup>2</sup>	mL CH <sub>4</sub> /g VS <sub>in</sub>	310 ± 6	-	226 ± 2
Total volatile solids reduction <sup>3</sup>	%		55 ± 7	

<sup>1</sup> Volatile solid reduction was calculated as  $(VS_{in}-VS_{out})/VS_{in}$

<sup>2</sup> BMP tests were performed on grab samples from the feed of D1a and D2 taken in October 2020

<sup>3</sup>  $VSR_{Total} = (VSR_{1^{st} \text{ stage}} + VSR_{2^{nd} \text{ stage}})/VS_{in, 1^{st} \text{ stage}}$

197

198 The values for Daily VS load, VS reduction and methane yield of second-stage digester (D2) are  
 199 affected by underestimation of volatile solids content of thermally treated sludge. Previous studies  
 200 have indicated that VS measurements in thermally treated sludge underestimate the actual volatile  
 201 solids content of sludge due to evaporation of VFAs, ammonia and other volatile short-chain products  
 202 at drying temperature (105°C) (Kreuger et al., 2011; Panter, 2008). The mean methane yield of D2  
 203 was  $379 \pm 66$  mL CH<sub>4</sub>/g VS<sub>in</sub>, which was higher than that obtained from BMP test  $226 \pm 2$   
 204 mL CH<sub>4</sub>/g VS<sub>in</sub>. The latter is similar to the value of 236 mL CH<sub>4</sub>/g VS<sub>in</sub> obtained for anaerobic  
 205 digestion of thermally treated digested sludge reported by Filer (2019). The overestimation of the  
 206 biogas flow rate can also be caused by deposits of elemental sulfur on the flowrate sensors generated  
 207 from microaeration, estimated by operators in the range of ~20%. The latter explanation might be  
 208 more plausible because the same VS measurement procedure was followed in the plant and for the  
 209 BMP test.

### 210 **3.2 Total sulfur content and fractionation in and out anaerobic digesters**

211 The total sulfur concentrations of anaerobic digesters (D1a and D2) are shown in Table 2. During the  
 212 seven-week measurement campaign C1 (2018), the total sulfur concentrations in the inlet and outlet of  
 213 D1a were  $9.5 \pm 2.6$  mg S/g DS and  $11.6 \pm 2.7$  mg S/g DS, respectively. The increase of sulfur  
 214 concentrations (mg S/kg Dry solids) after anaerobic digestion is linked to decrease of organic matter  
 215 that is converted into biogas in the anaerobic digester, causing the decrease of total solids (Dewil et al.,  
 216 2006). The few replicates of total sulfur measurements performed in 2019 and 2020 fall within the  
 217 standard deviation of the measurements performed in 2018. The total sulfur concentration in the  
 218 digested sludge of D1a was similar to those reported by Fisher et al. (2017). The total sulfur  
 219 concentration measurements in D2 were relatively similar, with lower standard deviation compared to  
 220 D1a, which can be attributed to more stable sludge characteristics and sulfur content.

221 Table 2: Mean and standard deviation of total sulfur concentrations as mg S/g of dry solids (DS) in  
 222 sludge treatment line. C1, C2 and C3 refer to the measurement campaigns in 2018, 2019 and 2020,  
 223 respectively. Values in parentheses represent the number of analyses in each period.

	D1 <sub>a</sub> <sup>feed</sup> mg S/g DS	D1 <sub>a</sub> <sup>outlet</sup> mg S/g DS	D2 <sup>feed</sup> mg S/g DS	D2 <sup>outlet</sup> mg S/g DS
C1 (2018)	9.5 ± 2.6 (n=22)	11.6 ± 2.7 (n=7)	12.3 ± 1.0 (n=6)	12.4 ± 1.5 (n=6)
C2 (2019)	7.9 ± 0.5 (n=3)	9.8 (n=2)	10.9 ± 0.3 (n=4)	12.9 ± 0.6 (n=4)
C3 (2020)	7.2 (n=2)	11.7 (n=2)	12.7 (n=2)	12.7 (n=2)

TPS: thickened primary sludge; TWAS: thickened waste activated sludge

224

225 The total sulfur mass flow decreased during both first stage (D1a) and second stage (D2) digestion  
 226 (Table 3). In D1a, total sulfur flows decreased from 139 ± 12 kg S/d in the inlet to 117 ± 13 kg S/d in  
 227 digested sludge. The total sulfur flow in the biogas (as H<sub>2</sub>S) accounted for 6.3 ± 1.2 kg S/d. It is  
 228 important to note that recorded H<sub>2</sub>S in the biogas is smaller to the actual total amount of H<sub>2</sub>S emitted  
 229 because part of H<sub>2</sub>S is oxidised to elemental sulfur through microaeration. Based on sulfur mass flows  
 230 in D1a, the gap in sulfur balance was ~11% (16 kg S/d), which could be attributed to elemental sulfur  
 231 deposits in the headspace and accumulated sulfur in the reactor. In addition, this value is within the  
 232 standard deviation of the measurements. Given the complexity of sampling from full-scale anaerobic  
 233 digesters and system fluctuations during measurement campaigns, the mass balances could be  
 234 considered as closed within acceptable range. In case of D2, sulfur flow in the feed decreased from  
 235 165 ± 12 kg S/d to 149 kg S/d in digested sludge and 9.2 ± 0.8 kg S/d H<sub>2</sub>S in biogas, implying a 4%  
 236 gap in sulfur mass flows.

237 Table 3: Average and standard deviation of total, particulate, and soluble sulfur mass flow as kg S/d in  
 238 the inlet, outlet and biogas of D1a and D2. The organic fraction of sulfur in the total sample and  
 239 particulate fraction is also given for D1a and D2. Values in parentheses represent the number of  
 240 samples analysed, n.

		D1 <sub>a</sub> <sup>feed</sup>	D1 <sub>a</sub> <sup>outlet</sup>	D1 <sub>a</sub> <sup>biogas</sup>	D2 <sup>feed</sup>	D2 <sup>outlet</sup>	D2 <sup>biogas</sup>
Total sulfur (S <sub>Total</sub> )	kg S/d	139 ± 12*	117 ± 13	6.3 ± 1.2	165 ± 12	149 ± 9	9.2 ± 0.8
	mg S/L	501 ± 42	422 ± 43	908 ± 107 (ppm)	1146 ± 58	1035 ± 33	1533 ± 68 (ppm)
Particulate sulfur (S <sub>Particulate</sub> )	kg S/d	119 ± 13	107 ± 13		110 ± 8	111 ± 10	

	mg S/L	431 ± 45	385 ± 44	762 ± 42	770 ± 56
Soluble sulfur ( $S_{\text{Soluble}}$ )	kg S/d	19 ± 2	10 ± 0.4	55 ± 4	38 ± 6
	mg S/L	70 ± 6	37 ± 1	384 ± 19	266 ± 40
<b>Fractionation (%)</b>					
$S_{\text{Organic}}/S_{\text{Total}}$ (OSF)		76 ± 3	68 ± 6	72 ± 3	58 ± 6
		(n=22)	(n=6)	(n=6)	(n=5)
$S_{\text{Particulate\_organic}}/S_{\text{Particulate}}$ (POSF)		77 ± 4	66 ± 5	60 ± 6	54 ± 6
		(n=6)	(n=5)	(n=7)	(n=6)

\* Mean ± standard error of the mean

241

242 The fractionations of soluble and particulate sulfur were different for the inlet of D1a and D2 (Table

243 3). The majority of sulfur in raw sludge entering D1a was in particulate fraction (~85%), while in

244 thermally treated sludge ( $D2_{\text{feed}}$ ) the particulate fraction of sulfur was lower (66%) resulting in

245 elevated soluble fraction (34%). The elevated fraction of soluble sulfur after thermal hydrolysis was

246 also observed in the measurements performed during C2 (41%, see Fig. A3 in SI). In addition to

247 sulfur, elevated soluble fraction in thermally treated sludge was detected for COD (47% and 31% for

248 C2 and C3, respectively, see Fig. A3 in SI). The measurement of organic and inorganic sulfur revealed

249 that total sulfur in raw sludge was mostly in organic fraction (76%). The lowest organic sulfur fraction

250 was observed in the final stage of treatment (i.e.  $D2_{\text{digested}} = 58 \pm 6\%$ ). Based on sulfur fractionation in

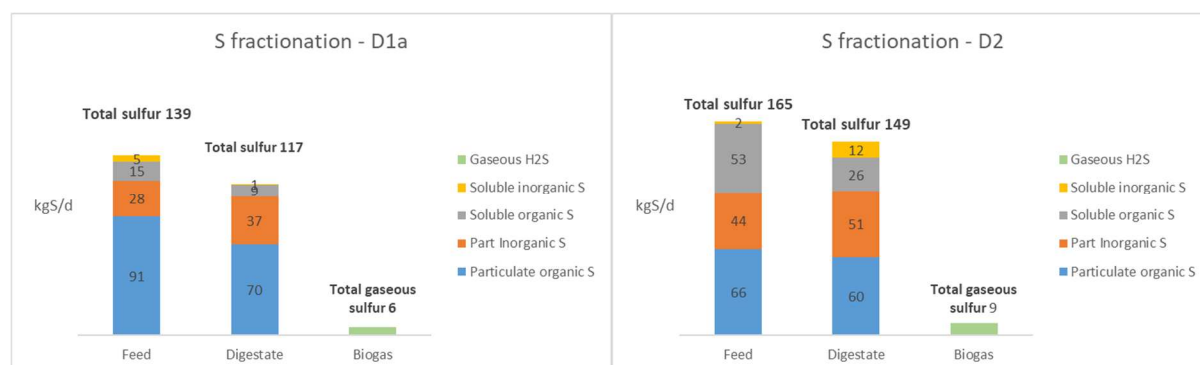
251 Table 3, the fate of soluble/particulate organic/inorganic sulfur in D1a and D2 can be deduced (Fig. 2).

252 From Fig. 2, it is apparent that the mass of total organic sulfur (i.e. sum of soluble and particulate

253 organic sulfur) decreased in both stages of digestion. The decrease in D1a and D2 are equal to 27 kg

254 S/d and 33 kg S/d, respectively. In D1a, the uptake of particulate organic sulfur was significant (21 kg

255 S/d), while in D2 the uptake of soluble organic sulfur was more pronounced (27 kg S/d).



256

257 Fig 2: Fate of soluble/particulate organic/inorganic sulfur in D1a and D2, calculated from the  
 258 fractionations given in Table 3.

259 Particulate inorganic sulfur increased after D1a and D2 with +9 and +7 kg S/d, respectively. Soluble  
 260 inorganic sulfur decreased in D1a (-4 kg S /d) but increased in D2 (+10 kg S/d). The evaluation of  
 261 soluble inorganic sulfur in anaerobic digestion is complex. First, accounting for the lowest fraction of  
 262 sulfur, soluble inorganic sulfur lies within the standard deviation of other fractions, thus these data  
 263 have to be interpreted with caution. Moreover, the behaviour of soluble sulfur species are different in  
 264 anaerobic digestion. For instance, while sulfate concentration is generally reduced due to the activity  
 265 of SRBs, the concentration of soluble sulfide might experience increase or decrease in effluent  
 266 according to several factors such as pH of the reactor and presence of soluble metals.

### 267 3.3 Contribution of biological sulfate reduction to H<sub>2</sub>S formation

268 To estimate the contribution of biological sulfate reduction to sulfide production, anaerobic digestion  
 269 batch experiments were performed on the samples taken from inlet of D1a and D2. The initial and  
 270 final concentrations of sulfate and soluble iron as well as cumulative concentration of H<sub>2</sub>S in biogas  
 271 are provided in Table 4. Sulfate concentrations were used to estimate the contribution of sulfate  
 272 reduction to the formation of sulfide. Sulfide formation were the sum of sulfide precipitated with  
 273 soluble iron as FeS and H<sub>2</sub>S emitted to biogas.

274 Table 4: Concentration for sulfate, soluble iron and gaseous H<sub>2</sub>S in batch experiments.

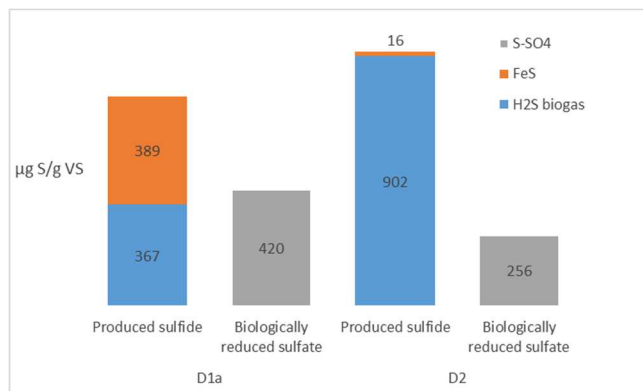
	<b>D1a<sub>feed</sub></b>	<b>D1a<sub>outlet</sub></b>	<b>D1a<sub>biogas</sub></b>	<b>D2<sub>feed</sub></b>	<b>D2<sub>outlet</sub></b>	<b>D2<sub>biogas</sub></b>
Sulfate (mg S/L)	12.9	1.4		12.5	6.0	
Soluble Fe (mg /L)	21	0.5		1.7	0.5	
Gaseous H <sub>2</sub> S in biogas (mL at STP*)			0.434 ± 0.044			1.185 ± 0.102

\*Standard temperature and pressure

275

276 In anaerobic digestion batch experiments (Fig. 3), sulfide produced from the biological reduction of  
 277 sulfate accounted for 56% (420 µg S/g VS<sub>in</sub> /756 µg S/g VS<sub>in</sub>) and 28% (256 µg S/g VS<sub>in</sub>/918 µg  
 278 S/g VS<sub>in</sub>) of total sulfide in D1a and D2, respectively. This result indicates that sulfate reduction would  
 279 not be the only mechanism contributing to sulfide production in D1a. The contribution of biological  
 280 sulfate reduction was much lower for the thermally treated sludge, since sulfate reduction only

281 accounts for 28% of sulfide production. It is important to bear in mind that other forms of sulfide (e.g.  
 282 soluble sulfide remained in effluent and precipitated sulfide with other metals) were not included;  
 283 therefore, produced sulfide could be lower than the actual total sulfide.



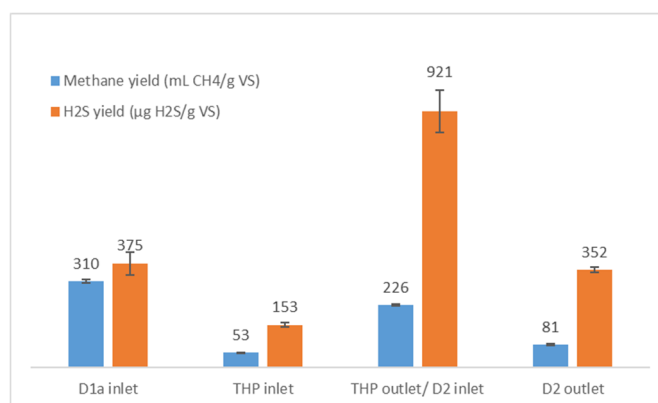
284  
 285 Fig 3: Comparison between sulfide production (either as H<sub>2</sub>S in biogas or precipitated FeS) and  
 286 biological sulfate reduction, for both first stage (D1a) and second-stage (D2) digestion. Values  
 287 obtained from batch tests.

288 Based on these results, it was then assessed whether the degradation of sulfur-containing amino acids  
 289 (cysteine and methionine) could explain the remaining difference between sulfide production and  
 290 biologically reduced sulfate. Because methionine and cysteine were not analysed in this study, their  
 291 concentrations in raw sludge and degradation rates in anaerobic digestion that were reported by Chen  
 292 et al. (2019) were used (See SI section A4). Indeed, these authors have reported the content of  
 293 hydrolytic cysteine and methionine in raw sludge as  $0.46 \pm 0.01$  mg/g dry sludge and  $3.60 \pm 0.01$  mg/g  
 294 dry sludge, respectively. In addition, the reported removal rate of cysteine and methionine in lab-scale  
 295 anaerobic digestion was  $34.78 \pm 7.87\%$  and  $48.06 \pm 0.77\%$ , respectively. With these values, the  
 296 contribution of cysteine and methionine to the formation of sulfide were calculated, as  $62 \mu\text{g S/ g VS}_{\text{in}}$   
 297 and  $542 \mu\text{g S/ g VS}_{\text{in}}$ , respectively, leading to a total potential sulfide formation of  $1023 \mu\text{g S/ g VS}_{\text{in}}$ .  
 298 Although the calculated potential sulfide formation is higher than the measured sulfide ( $756 \mu\text{g S/ g}$   
 299  $\text{VS}_{\text{in}}$ ), these values are in the same order of magnitude. The difference could be explained by the fact  
 300 that we did not measure all sulfide (remaining soluble sulfide and sulfide precipitated with other

301 metals). Nevertheless, this result supports our previous statement that the degradation of organic sulfur  
302 is a major mechanism for the formation of H<sub>2</sub>S in anaerobic digestion.

### 303 **3.4 Profile of methane yield and H<sub>2</sub>S in biogas of batch anaerobic digestion**

304 H<sub>2</sub>S formation and methane yield during anaerobic digestion batch experiments of samples taken from  
305 various stages are given in Fig. 4. The yield of H<sub>2</sub>S dramatically increased from 153 μg H<sub>2</sub>S/g VS<sub>in</sub> to  
306 921 μL H<sub>2</sub>S/ g VS<sub>in</sub> because of thermal hydrolysis. The increase is partially caused by the sulfate  
307 content (20-40 mg S/L) of the treated effluent which was added to the thermally treated sludge for  
308 dilution and cooling. Interestingly, the H<sub>2</sub>S yield of digested sludge (D2<sub>outlet</sub>) remained noticeable (352  
309 μg H<sub>2</sub>S/g VS<sub>in</sub>). The methane yield also increased considerably from 53 mL CH<sub>4</sub>/g VS<sub>in</sub> in the inlet to  
310 226 mL CH<sub>4</sub>/g VS<sub>in</sub> in thermally treated sludge.



311  
312 Fig 4: Profile of gaseous methane yield (mL CH<sub>4</sub>/g VS) and hydrogen sulfide yield (μg H<sub>2</sub>S/ g VS) in  
313 the different stages.

## 314 **4 Discussion**

### 315 **4.1 Operational assessment of two-stage anaerobic digestion**

316 In a two-stage anaerobic digestion with intermediate thermal hydrolysis (also referred to DLD  
317 configuration), the first digestion stage should have similar operational and performance behaviours to  
318 typical one-stage anaerobic digestion. It was confirmed by the calculated methane yield of D1a using  
319 long-term dataset which corresponded to typical methane yields reported for mesophilic anaerobic  
320 digestions (Bachmann et al., 2015). On the other hand, the literature on second digestion stage located

321 after thermal hydrolysis is relatively scarce. The performance evaluation of second digestion stage, in  
322 particular the parameters related to biogas flow rate and VS measurements (i.e. VS reduction, methane  
323 yield) was complex. A number of authors have reported that the assessment of volatile solids by  
324 standard weight loss after drying is often difficult for samples containing a large fraction of soluble  
325 organic material (Beall et al., 1998; Kreuger et al., 2011; Panter, 2008), due to the volatilisation of  
326 soluble components during solids drying at 105°C that would otherwise be considered volatile solids  
327 (e.g. VFA and ammonia). This loss results in an artificially low sludge dry solid content in hydrolysed  
328 sludge, hence low volatile matter content. According to Panter (2008), this underestimation is more  
329 intensified in case of thermally treated sludge, which can account for up to a loss of 1% DS, i.e. 10%  
330 DS measured is actually 11% total solids, and a solution would be DS and VS measurement in the raw  
331 cake (i.e. inlet of thermal hydrolysis). In this study, the long-term comparison of dry solids in the inlet  
332 and outlet of thermal hydrolysis showed an average of  $15 \pm 7\%$  lower DS in the thermally treated  
333 sludge. When using the measurement of the dry solids in the inlet of thermal hydrolysis, the calculated  
334 methane yield of D2 decreased from  $379 \pm 66$  mL CH<sub>4</sub>/ g VS<sub>in</sub> to  $314 \pm 58$  mL CH<sub>4</sub>/ g VS<sub>in</sub>, and VS  
335 reduction increased from  $32 \pm 5\%$  to  $43 \pm 6\%$ . Further research is needed to assess the emission of  
336 volatile organic compounds in the off-gas stream of the thermal hydrolysis process.

## 337 **4.2 The effect of intermediate thermal hydrolysis on organic matter**

### 338 **solubilisation, methane production, and H<sub>2</sub>S production**

339 Intermediate thermal hydrolysis focuses on the solubilisation of hard to digest fraction of sludge  
340 during first anaerobic digestion, making them more degradable in the second stage digester (Abu-Orf  
341 and Goss, 2012; Shana et al., 2015). The results obtained from full-scale thermal hydrolysis in this  
342 study demonstrated the efficiency of this process unit in solubilising organic matter, which is typically  
343 measured by the degree of solubilisation determined as soluble COD relative to the total COD. The  
344 soluble fraction of COD in thermally treated sludge obtained in this study (47% and 31% for C2 and  
345 C3, respectively) was similar to the prior findings in lab-scale experiments (Han et al., 2017; Wett et  
346 al., 2009; Xue et al., 2015), although these authors obtained the values for thermal treatment of raw  
347 sludge. The biodegradability improvement due to thermal treatment is supported by the results of

348 BMP tests, where a 327% (i.e. from  $53 \pm 1.6$  to  $226 \pm 1.9$  ml CH<sub>4</sub>/ g VS<sub>in</sub>, Fig. 4) increase in methane  
349 yield of the digested cake was obtained after thermal hydrolysis.

350 Similarly, the elevated soluble fraction of sulfur in thermally treated sludge (34% and 41% of total  
351 sulfur for C1 and C2, respectively) could be attributed to the solubilisation of protein as the largest  
352 fraction of wastewater organic material (Wilson and Novak, 2009), which is also the major contributor  
353 to organic sulfur (Du and Parker, 2013). The organic origin of soluble sulfur in thermally treated  
354 sludge is also supported by sulfur fractionations given in Table 3. It is also consistent with the findings  
355 of Han et al. (2017) that reported minor variation of inorganic sulfur (i.e. sulfate, soluble sulfide, and  
356 particulate sulfide) during thermal hydrolysis. Solubilisation of sulfur-bearing organics, likely protein,  
357 during thermal hydrolysis resulted in an increase in the biodegradability of organic sulfur, which could  
358 be clearly seen by comparing the H<sub>2</sub>S production in anaerobic digestion batch experiments of sample  
359 taken from thermally treated sludge to that of digested cake entering thermal hydrolysis.

### 360 **4.3 Influence of organic sulfur on the formation of H<sub>2</sub>S**

361 In municipal anaerobic digestion, H<sub>2</sub>S is generated from the biological sulfate reduction and organic  
362 sulfur degradation. Sulfur containing amino acids (Cysteine and methionine) are the main source of  
363 organic sulfur in sludge (Sommers et al., 1977) which are reported to be source of H<sub>2</sub>S and other  
364 volatile organic sulfur compounds (e.g. methyl mercaptan, dimethyl sulfide and dimethyl disulphide).  
365 Cysteine is considered as an organic precursor of only H<sub>2</sub>S under anaerobic conditions, while  
366 methionine is reported to be degraded through different pathways under different conditions to  
367 produce either methyl mercaptan, dimethyl sulfide or H<sub>2</sub>S. VOSC concentrations in digesters are  
368 reduced by methanogens that mediate the degradation of VOSC to H<sub>2</sub>S (Du and Parker, 2012). While  
369 a considerable amount of literature has been published on biological sulfate reduction, focusing on  
370 sulfate-rich wastewater, the influence of organic sulfur fraction on the formation of H<sub>2</sub>S and other  
371 volatile organic sulfur compounds has been rarely reported. The results obtained in this study enabled  
372 to elucidate the fate of organic sulfur in two-stage anaerobic digestion with intermediate thermal  
373 hydrolysis.

374 Organic sulfur fraction accounted for the majority of total sulfur in mixed primary and secondary  
375 sludge entering first anaerobic digestion stage (Table 3). In the first digestion stage the uptake of  
376 organic sulfur was 25% (Table 3, calculated as relative difference of organic sulfur in the inlet and  
377 outlet of D1a), mostly affected by the particulate organic sulfur. This behaviour could be explained by  
378 the low fraction of soluble organics in raw sludge due to preceding thickening process units. The  
379 increase of particulate inorganic sulfur was as expected because of precipitation of sulfide with metals  
380 (e.g.  $\text{Fe}^{2+}$ ) and the presence of elemental sulfur in digested sludge. Interestingly, the increase in  
381 particulate inorganic sulfur (i.e. metal sulfide) was inferior to organic uptakes in D1a, indicating the  
382 role of organic sulfur uptake in production of sulfide, which could be emitted as  $\text{H}_2\text{S}$  or remained in  
383 the liquid phase as soluble sulfide given the condition of anaerobic digestion (i.e. pH).

384 Further investigation of total sulfide formation in anaerobic digestion batch experiments of raw sludge  
385 demonstrated the importance of organic sulfur uptake in the formation of sulfide as biological sulfate  
386 reduction only accounted for 56% of the total amount of sulfide produced (Fig. 3). The literature on  
387 the fate of organic sulfur in anaerobic digestion is relatively scarce, however, from the recent  
388 published works, it can be hypothesised that organic sulfur mostly from primary sludge and sulfate  
389 contributed to the formation of  $\text{H}_2\text{S}$  in the first digestion stage. According to Du and Parker (2013) the  
390 sulfur-containing organic matter in primary sludge are more degradable during anaerobic digestion  
391 than that of secondary sludge. The higher degradation of organics in primary sludge is consistent with  
392 recent findings that observed a strong correlation between the volatile solids in primary sludge and  
393 concentration of  $\text{H}_2\text{S}$  in biogas of full-scale municipal anaerobic digestion (Erdirencelebi and  
394 Kucukhemek, 2018).

395 In the second digestion stage, the role of organic sulfur in the total sulfide production is even more  
396 pronounced. Indeed, the uptake of soluble organic sulfur was substantial, with a 50% reduction in  
397 mass flows (Table 3). Moreover, anaerobic digestion batch tests of thermally treated sludge showed  
398 that biological sulfate reduction only explained 28% of total sulfide formed during the experiment.  
399 This result demonstrates the undeniable role of organic sulfur uptake for  $\text{H}_2\text{S}$  formation. It is reported  
400 that sulfur-containing organics in secondary sludge present as biomass proteins are not fully

401 degradable in anaerobic digestion due to their large molecular size (Du and Parker, 2013), but become  
402 more degradable during thermal hydrolysis due to the disruption of cell walls and even smaller  
403 fractions such as amino acids (Remy and Diercks, 2016). Indeed, the majority of sulfur in thickened  
404 secondary sludge is in organic form ~90% in this study (data not shown). In our batch tests, the 500%  
405 increase of H<sub>2</sub>S yield of the samples before and after thermal hydrolysis supported this argument. The  
406 data collected from full-scale digestion and batch experiments are consistent in indicating that the  
407 uptake of organic sulfur, especially in the anaerobic digestion of thermally treated sludge (D2) plays  
408 an important role in the generation of sulfide.

409 The above-described fate of organic sulfur needs further investigation to improve speciation of organic  
410 sulfur compounds and their transformations in anaerobic digestion by development of measurement  
411 techniques. Failing to accurately predict H<sub>2</sub>S production in municipal anaerobic digestion causes  
412 severe problems including corruptions, lower biogas production, lower biogas profitability due to  
413 applying costly H<sub>2</sub>S treatment methods (e.g. activated carbons).

#### 414 **4.4 Incorporating sulfur reactions in anaerobic digestion**

415 Several models have been developed to include the transformation of sulfur species during anaerobic  
416 digestion process, reported in a number of studies (Barrera et al., 2015; D'Acunto et al., 2011;  
417 Fedorovich et al., 2003; Flores-Alsina et al., 2016; Hauduc et al., 2018; Poinapen and Ekama, 2010;  
418 Solon et al., 2017). In these models, H<sub>2</sub>S is generated solely from biological reduction of sulfate by  
419 SRBs, while the contribution of organic sulfur to H<sub>2</sub>S is not included. While this assumption could be  
420 acceptable for anaerobic digestion of sulfate-rich wastewater, which has been the case for majority of  
421 models, the results of this study indicates that biological sulfate reduction leads to underestimation of  
422 sulfide production in anaerobic digestion of municipal WWTPs. The result of this study also showed  
423 that solubilisation and hydrolysis of organic sulfur during thermal hydrolysis process substantially  
424 increased the generation of H<sub>2</sub>S during anaerobic digestion process. This effect, to our knowledge, has  
425 not yet been addressed into modelling studies. Some software packages such as Sumo<sup>®</sup> (Dynamita)  
426 have incorporated the conversions of organic sulfur during anaerobic digestion, however, their  
427 modelling approach, assumptions and kinetics are not well described.

## 428 **5 Conclusions**

429 The fate of organic and inorganic sulfur compounds during two-stage anaerobic digestion with  
430 intermediate thermal hydrolysis was investigated through a seven-week, full-scale measuring  
431 campaign, complemented with batch experiments.

- 432 • Intermediate thermal hydrolysis effectively improved the solubilisation and thus  
433 biodegradability of digested sludge that resulted in significant increase in both methane yield  
434 and H<sub>2</sub>S production in thermally treated sludge.
- 435 • The uptake of organic sulfur during both anaerobic digestion stages was found non-negligible.  
436 The converted organic sulfur in the first digester was mostly in particulate form, while  
437 converted organic sulfur in the second digester, following thermal hydrolysis, was mostly  
438 soluble.
- 439 • Sulfate reduction could not explain all sulfide produced during anaerobic digestion. This effect  
440 was even more pronounced for thermally treated sludge. Batch digestion experiments  
441 indicated that biological sulfate reduction accounted for 56% and 28% of total sulfide (H<sub>2</sub>S in  
442 biogas and precipitated FeS) produced in the first and second stages of digestion respectively.
- 443 • The results dispute sulfate as the single contributor to H<sub>2</sub>S formation during anaerobic  
444 digestion. H<sub>2</sub>S formation from organic sulfur conversion is significant; its share increases  
445 through thermal hydrolysis.

## 446 **6 Acknowledgements**

447 This work was performed within the framework of the EUR H2O'Lyon (ANR-17-EURE-0018) of  
448 Université de Lyon (UdL), within the program "Investissements d'Avenir" operated by the French  
449 National Research Agency (ANR). The work of Kimberly Solon was supported by the Research  
450 Foundation Flanders (FWO) through an ERC runner-up project for Eveline Volcke and by European  
451 Union's Horizon 2020 research and innovation programme under the Marie Skłodowska-Curie Grant  
452 Agreement No. 846316 (WISEFLOW). The authors thank Sylvain Chastrusse, Christophe Renner,

453 Jonathan Coulmin, Vanessa Gromand, Ian Garcia-Fernandez from Veolia for facilitating and carrying  
454 out the measurement campaign.

## 455 **7 References**

456 Abu-Orf, M., Goss, T., 2012. Comparing Thermal Hydrolysis Processes (CAMBI™ and EXELYS™)  
457 For Solids Pretreatment Prior To Anaerobic Digestion. *Digestion* 16, 8–12.

458 Ahmed, W., Rodríguez, J., 2018. Modelling sulfate reduction in anaerobic digestion: Complexity  
459 evaluation and parameter calibration. *Water Res.* 130, 255–262.

460 Amodeo, C., Hafner, S.D., Franco, R.T., Benbelkacem, H., Moretti, P., Bayard, R., Buffière, P., 2020.  
461 How Different are manometric, gravimetric, and automated volumetric BMP results? *Water*  
462 (Switzerland) 12.

463 Appels, L., Baeyens, J., Degreè, J., Dewil, R., 2008. Principles and potential of the anaerobic  
464 digestion of waste-activated sludge. *Prog. Energy Combust. Sci.* 34, 755–781.

465 Bachmann, N., la Cour Jansen, J., Bochmann, G., Montpart, N., 2015. Sustainable biogas production  
466 in municipal wastewater treatment plants. IEA Bioenergy Massongex, Switzerland.

467 Barber, W.P.F., 2016. Thermal hydrolysis for sewage treatment: A critical review. *Water Res.* 104,  
468 53–71.

469 Barrera, E.L., Spanjers, H., Dewulf, J., Romero, O., Rosa, E., 2013. The sulfur chain in biogas  
470 production from sulfate-rich liquid substrates: A review on dynamic modeling with vinasse as  
471 model substrate. *J. Chem. Technol. Biotechnol.* 88, 1405–1420.

472 Barrera, E.L.L., Spanjers, H., Solon, K., Amerlinck, Y., Nopens, I., Dewulf, J., 2015. Modeling the  
473 anaerobic digestion of cane-molasses vinasse: Extension of the Anaerobic Digestion Model No.  
474 1 (ADM1) with sulfate reduction for a very high strength and sulfate rich wastewater. *Water Res.*  
475 71, 42–54.

476 Beall, S.S., Jenkins, D., Vidanage, S.A., 1998. A systematic analytical artifact that significantly

477 influences anaerobic digestion efficiency measurement. *Water Environ. Res.* 70, 1019–1024.

478 Chen, S., Dong, B., Dai, X., Wang, H., Li, N., Yang, D., 2019. Effects of thermal hydrolysis on the  
479 metabolism of amino acids in sewage sludge in anaerobic digestion. *Waste Manag.* 88, 309–318.

480 Chen, Y., Adams, G., Erdal, Z., Forbes, R.H., Hargreaves, R., Higgins, M.J., Murthy, S.N., Novak,  
481 J.T., Witherspoon, J., Toffey, W.E., 2007. The effect of aluminum sulfate addition during  
482 condition on production of volatile organic sulfur compounds from anaerobically digested  
483 biosolids. *Water Pract.* 1, 1–13.

484 Chen, Y.C., Higgins, M.J., Beightol, S.M., Murthy, S.N., Toffey, W.E., 2011. Anaerobically digested  
485 biosolids odor generation and pathogen indicator regrowth after dewatering. *Water Res.* 45,  
486 2616–2626.

487 D’Acunto, B., Esposito, G., Frunzo, L., Pirozzi, F., Acunto, B.D., Esposito, G., Frunzo, L., Pirozzi, F.,  
488 2011. Dynamic modeling of sulfate reducing biofilms. *Comput. Math. with Appl.* 62, 2601–  
489 2608.

490 Dewil, R., Baeyens, J., Roels, J., Steene, B. Van De, 2009. Evolution of total sulphur content in full  
491 scale wastewater sludge treatment. *Environ. Eng. Sci.* 26, 292–300.

492 Dewil, R., Baeyens, J., Roels, J., Steene, B. Van De, 2008. Distribution of sulphur compounds in  
493 sewage sludge treatment. *Environ. Eng. Sci.* 25, 879–886.

494 Dewil, R., Baeyens, J., Roelandt, F., & Peereman, M. 2006. The analysis of the total sulphur content  
495 of wastewater treatment sludge by ICP-OES. *Environ. Eng. Sci.* 23, 904-907.

496 Donoso-Bravo, A., Mailier, J., Martin, C., Rodríguez, J., Aceves-Lara, C.A., Wouwer, A. Vande,  
497 2011. Model selection, identification and validation in anaerobic digestion: A review. *Water Res.*  
498 45, 5347–5364.

499 Du, W., Parker, W., 2013. Characterization of sulfur in raw and anaerobically digested municipal  
500 wastewater treatment sludges. *Water Environ. Res.* 85, 124–132.

501 Du, W., Parker, W., 2012. Modeling volatile organic sulfur compounds in mesophilic and

502 thermophilic anaerobic digestion of methionine. *Water Res.* 46, 539–546.

503 Erdal, Z.K., Forbes, R.H., Witherspoon, J., Adams, G., Hargreaves, R., Morton, R., Novak, J.,  
504 Higgins, M., 2008. Recent findings on biosolids cake odor reduction - Results of WERF phase 3  
505 biosolids odor research. *J. Environ. Sci. Heal. - Part A Toxic/Hazardous Subst. Environ. Eng.* 43,  
506 1575–1580.

507 Erdirencelebi, D., Kucukhemek, M., 2018. Control of hydrogen sulphide in full-scale anaerobic  
508 digesters using iron (Iii) chloride: Performance, origin and effects. *Water SA* 44, 176–183.

509 Fedorovich, V., Lens, P., Kalyuzhnyi, S., 2003. Extension of Anaerobic Digestion Model No . 1 with  
510 Processes of sulfate reduction. *Appl. Biochem. Biotechnol.* 109, 33–45.

511 Filer, J., 2019. Anaerobic digestion system incorporating intermediate thermal treatment: a laboratory  
512 scale investigation into enhancing methane productivity. Ph.D. thesis, University of Guelph,  
513 Canada.

514 Fisher, R.M., Alvarez-Gaitan, J.P., Stuetz, R.M., Moore, S.J., 2017. Sulfur flows and biosolids  
515 processing: Using Material Flux Analysis (MFA) principles at wastewater treatment plants. *J.*  
516 *Environ. Manage.* 198, 153–162.

517 Flores-Alsina, X., Solon, K., Mbamba, C.K., Tait, S., Gernaey, K. V., Jeppsson, U., Batstone, D.J.,  
518 Kazadi Mbamba, C., Tait, S., Gernaey, K. V., Jeppsson, U., Batstone, D.J., 2016. Modelling  
519 phosphorus (P), sulfur (S) and iron (Fe) interactions for dynamic simulations of anaerobic  
520 digestion processes. *Water Res.* 95, 370–382.

521 Forouzanmehr F., Le Q.H., Solon K., Maisonnave V., Daniel O., Buffiere P., Gillot S., Volcke E.I.P.,  
522 Plant-wide investigation of sulfur flows in a water resource recovery facility (WRRF). *Science of*  
523 *the Total Environment*, 801, 149530.

524 Han, Y., Zhuo, Y., Peng, D., Yao, Q., Li, H., Qu, Q., 2017. Influence of thermal hydrolysis  
525 pretreatment on organic transformation characteristics of high solid anaerobic digestion.  
526 *Bioresour. Technol.* 244, 836–843.

527 Hauduc, H., Wadhawan, T., Johnson, B., Bott, C., Ward, M., Takács, I., 2018. Incorporating sulfur  
528 reactions and interactions with iron and phosphorus into a general plant-wide model. *Water Sci.*  
529 *Technol.* 79, 26–34.

530 Higgins, M.J., Adams, G., Chen, Y.-C., Erdal, Z., Forbes, R.H., Glindemann, D., Ronald Hargreaves,  
531 J., McEwen, D., Murthy, S.N., Novak, J.T., Witherspoon, J., 2008. Role of Protein, Amino  
532 Acids, and Enzyme Activity on Odor Production from Anaerobically Digested and Dewatered  
533 Biosolids. *Water Environ. Res.* 80, 127–135.

534 Higgins, M.J., Chen, Y., Yarosz, D.P., Murthy, S.N., Maas, N.A., Glindemann, D., Novak, J.T., 2006.  
535 Cycling of Volatile Organic Sulfur Compounds in Anaerobically Digested Biosolids and its  
536 Implications for Odors. *Water Environ. Res.* 78, 243–252.

537 Holliger, C., Alves, M., Andrade, D., Angelidaki, I., Astals, S., Baier, U., Bougrier, C., Buffière, P.,  
538 Carballa, M., De Wilde, V., Ebertseder, F., Fernández, B., Ficara, E., Fotidis, I., Frigon, J.C., De  
539 Laclos, H.F., Ghasimi, D.S.M., Hack, G., Hartel, M., Heerenklage, J., Horvath, I.S., Jenicek, P.,  
540 Koch, K., Krautwald, J., Lizasoain, J., Liu, J., Mosberger, L., Nistor, M., Oechsner, H., Oliveira,  
541 J.V., Paterson, M., Pauss, A., Pommier, S., Porqueddu, I., Raposo, F., Ribeiro, T., Pfund, F.R.,  
542 Strömberg, S., Torrijos, M., Van Eekert, M., Van Lier, J., Wedwitschka, H., Wierinck, I., 2016.  
543 Towards a standardization of biomethane potential tests. *Water Sci. Technol.* 74, 2515–2522.

544 Krayzelova, L., Bartacek, J., Kolesarova, N., Jenicek, P., 2014. Microaeration for hydrogen sulfide  
545 removal in UASB reactor. *Bioresour. Technol.* 172, 297–302.

546 Kreuger, E., Nges, I., Björnsson, L., 2011. Ensiling of crops for biogas production: Effects on methane  
547 yield and total solids determination. *Biotechnol. Biofuels* 4, 1–8.

548 Muller, C.D., Verma, N., Higgins, M.J., Novak, J.T., 2004. The role of shear in the generation of  
549 nuisance odors from dewatered biosolids. *Proc. Water Environ. Fed.* 2004, 376–388.

550 Novak, J.T., Adams, G., Chen, Y.-C., Erdal, Z., Forbes, R.H., Glindemann, D., Hargreaves, J.R.,  
551 Hentz, L., Higgins, M.J., Murthy, S.N., Witherspoon, J., 2006. Generation Pattern of Sulfur

552           Containing Gases from Anaerobically Digested Sludge Cakes. *Water Environ. Res.* 78, 821–827.

553 Panter, K., 2008. Mass balance and energy balance in high solid digestion following thermal  
554 hydrolysis pre-treatment, in: 13th European Biosolids and Organic Resources Conference and  
555 Workshop. November 10–12, Lancashire, UK.

556 Poinapen, J., Ekama, G.A., 2010. Biological sulphate reduction with primary sewage sludge in an  
557 upflow anaerobic sludge bed reactor - part 5: Steady-state model. *Water SA* 36, 193–202.

558 Remy, C., Diercks, K., 2016. POWERSTEP WP3 Biogas Valorization and Efficient Energy  
559 Management: Deliverable D3.1: Best practices for improved sludge digestion (Report No.  
560 RN1039). Kompetenzzentrum Wasser Berlin. [https://publications.kompetenz-](https://publications.kompetenz-wasser.de/pdf/Remy-2016-1039.pdf)  
561 [wasser.de/pdf/Remy-2016-1039.pdf](https://publications.kompetenz-wasser.de/pdf/Remy-2016-1039.pdf)

562 Shana, A.D., Ouki, S., Asaadi, M., Pearce, P., 2015. The impact of intermediate thermal hydrolysis  
563 process and conventional thermal hydrolysis process on biochemical composition during  
564 anaerobic digestion of sewage sludge, in: Proc., 20th European Biosolids and Organic Resources  
565 Conf. and Exhibition. November 9-11, Manchester, UK.

566 Solon, K., Flores-Alsina, X., Mbamba, C.K., Ikumi, D., Volcke, E.I.P., Vaneckhaute, C., Ekama, G.,  
567 Vanrolleghem, P.A., Batstone, D.J., Gernaey, K. V, 2017. Plant-wide modelling of phosphorus  
568 transformations in wastewater treatment systems: Impacts of control and operational strategies.  
569 *Water Res.* 113, 97–110.

570 Sommers, L.E., Tabatabai, M.A., Nelson, D.W., 1977. Forms of Sulfur in Sewage Sludge. *J. Environ.*  
571 *Qual.* 6, 42–46.

572 Svensson, K., Kjørlaug, O., Higgins, M.J., Linjordet, R., Horn, S.J., 2018. Post-anaerobic digestion  
573 thermal hydrolysis of sewage sludge and food waste: Effect on methane yields, dewaterability  
574 and solids reduction. *Water Res.* 132, 158–166.

575 Tang, K., Baskaran, V., Nemati, M., 2009. Bacteria of the sulphur cycle: an overview of microbiology,  
576 biokinetics and their role in petroleum and mining industries. *Biochem. Eng. J.* 44, 73–94.

577 Visser, A., 1995. The anaerobic treatment of sulfate containing wastewater. Ph. D. thesis, Wageningen  
578 Agriculture University, Netherlands.

579 Wett, B., Murthy, S.N., Takács, I., Wilson, C.A., Novak, J.T., Panter, K., Bailey, W., 2009. Simulation  
580 of thermal hydrolysis at the blue plains AWT: a new toolkit developed for full-plant process  
581 design. *Proc. Water Environ. Fed.* 2009, 2688–2698.

582 Wilson, C.A., Novak, J.T., 2009. Hydrolysis of macromolecular components of primary and  
583 secondary wastewater sludge by thermal hydrolytic pretreatment. *Water Res.* 43, 4489–4498.

584 Xue, Y., Liu, H., Chen, S., Dichtl, N., Dai, X., Li, N., 2015. Effects of thermal hydrolysis on organic  
585 matter solubilization and anaerobic digestion of high solid sludge. *Chem. Eng. J.* 264, 174–180.

586 Yang, G., Zhang, G., Zhuan, R., Yang, A., Wang, Y., 2016. Transformations, inhibition and inhibition  
587 control methods of sulfur in sludge anaerobic digestion: a review. *Curr. Org. Chem.* 20, 2780–  
588 2789.

589